nature structural & molecular biology

Alternative splicing of SYK regulates mitosis and cell survival

Panagiotis Prinos[1], Daniel Garneau[1], Jean-François Lucier[1], Daniel Gendron[1], Sonia Couture[1], Marianne Boivin[1], Jean-Philippe Brosseau[1,2], Elvy Lapointe[1], Philippe Thibault[1], Mathieu Durand[1], Karine Tremblay[1], Julien Gervais-Bird[1], Hanad Nwilati[1], Roscoe Klinck[1,3], Benoit Chabot[1,3], Jean-Pierre Perreault[2], Raymund J Wellinger[3] & Sherif Abou Elela[1,3]

Most human genes produce multiple mRNA isoforms through alternative splicing. However, the biological relevance of most splice variants remains unclear. In this study, we evaluated the functional impact of alternative splicing in cancer cells. We modulated the splicing pattern of 41 cancer-associated splicing events and scored the effects on cell growth, viability and apoptosis, identifying three isoforms essential for cell survival. Specifically, changing the splicing pattern of the spleen tyrosine kinase gene (SYK) impaired cell-cycle progression and anchorage-independent growth. Notably, exposure of cancer cells to epithelial growth factor modulated the SYK splicing pattern to promote the pro-survival isoform that is associated with cancer tissues *in vivo*. The data suggest that splicing of selected genes is specifically modified during tumor development to allow the expression of isoforms that promote cancer cell survival.

Currently, most therapeutic approaches define a target as one protein, one gene or one function. Yet whole-transcriptome sequencing has confirmed that only a minority of genes produce a single protein[1,2]. Indeed, the vast majority of genes use alternative splicing to produce several protein isoforms. In eukaryotes, alternative splicing has a central role both in protein diversity and in post-transcriptional gene regulation. Although alternative splicing can introduce or remove regulatory elements to affect translation, localization or degradation of an mRNA[3], in most cases it will produce multiple and functionally diverse protein isoforms[4]. Perturbations in alternative splicing are common and extensive in cancer[5] and can affect cancer development and maintenance[6]. For example, a switch in the alternative splicing of CD44 has been associated with the acquisition of metastatic potential[7]. Furthermore, a splicing switch in pyruvate kinase, a glycolytic enzyme, is essential for cancer metabolism and tumor growth[8]. However, the general impact of alternative splicing in cancer biology and its impact on drug targeting remain largely unexplored[9]. Indeed, it is not clear whether in many cases changing the proportion of a given set of splice variants may contribute to cancer biology independently of gene expression levels.

RNA interference (RNAi) has become a preferred tool for discovering and evaluating the impact of gene expression on the viability of cancer cells[10]. However, RNAi-based screens commonly target genes without considering the variety of alternative mRNA isoforms generated by alternative splicing. This limits our understanding of individual isoform functions and strongly reduces the numbers of potential drug targets. Our recent studies in ovarian[11] and breast cancer[12] identified 74 new cancer-associated splicing events. Here we describe a systematic isoform-specific functional screen of 41 alternatively spliced variants associated with breast and/or ovarian cancer, with the goal of evaluating the effect of alternative splicing on cancer biology. Our targeting approach uses a dual system for isoform-specific silencing and modulation. This comprehensive approach harnesses the power of small interfering RNA (siRNA) for isoform-specific silencing[13] and complements it with alternative splicing modulation using bifunctional antisense oligonucleotides[14]. Furthermore, this method uncouples the impact of splicing modulation on cell function from that of phenotypic defects caused by changes in gene expression levels. The results identify alternative splicing in genes associated with cell survival as important targets for breast and ovarian cancer. Changing the splicing pattern of the tyrosine kinase (SYK) altered cell survival and mitotic progression, whereas global knockdown of the same gene had no effect, suggesting that, at least for some genes, global knockdown of gene expression cannot mimic the effects of alternative splicing on cell survival and apoptosis.

RESULTS

Functional analysis of cancer-associated splice variants

Many alternative splicing events (ASEs) are modified in tumor cells[5]. However, little is known about the contribution of alternative splicing to cancer biology. To gain insight into this aspect of cancer, we have developed a platform for high-content functional analysis of alternative splicing events (FASE) (**Supplementary Fig. 1**) and have used it to examine the function of 29 ovarian[11] and 21 breast[12] cancer variants, including 9 that are common to both cancers (**Supplementary Table 1**). For a graphical representation of the protein domains affected in these variants, see http://palace.lgfus.ca/link/40_ases.

We classified these cancer-associated ASEs on the basis of their splicing pattern, and we then designed isoform-specific inhibitors for

[1]Laboratoire de Génomique Fonctionnelle, Université de Sherbrooke, Sherbrooke, Québec, Canada. [2]Département de Biochimie, Faculté de Médecine et des Sciences de la Santé, Université de Sherbrooke, Sherbrooke, Québec, Canada. [3]Département de Microbiologie et d'Infectiologie, Université de Sherbrooke, Sherbrooke, Québec, Canada. Correspondence should be addressed to S.A.E. (sherif.abou.elela@usherbrooke.ca).

Received 14 December 2010; accepted 17 February 2011; published online 8 May 2011; doi:10.1038/nsmb.2040

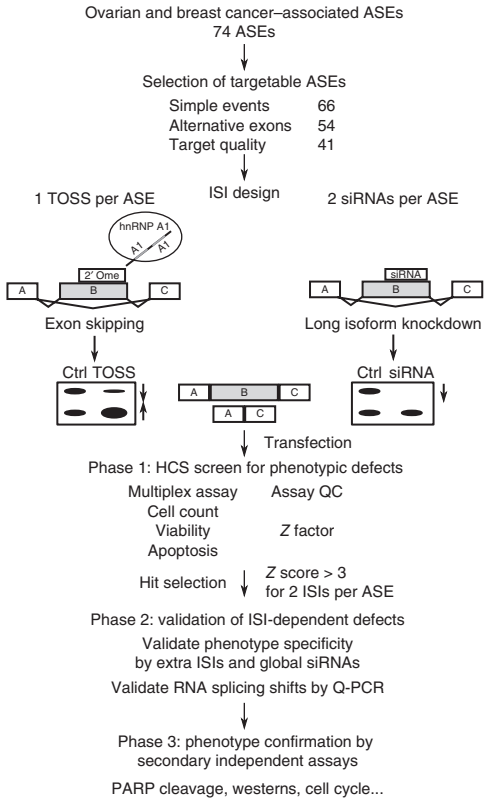

Figure 1 Strategy for functional annotation of cancer-associated ASEs. Ovarian cancer–associated and breast cancer–associated alternative cassette exons were identified and their expression was modulated using isoform-specific inhibitors (ISIs). Each simple alternative cassette exon or alternative 5′ splice site was inhibited using two independent exon-specific siRNAs, and its splicing was modulated using a TOSS. The impact of modulating the expression of splice isoforms on cell proliferation, viability and induction of apoptosis was monitored using the high-content FASE platform. Phenotypes caused by selective modulation of splice isoform ratios, and not the overall inhibition of gene expression, were considered indicators of alternative splicing isoform-specific functions.

all events with simple alternative 5′ events or cassette exons (**Fig. 1** and **Supplementary Fig. 2**). Two exon-specific siRNAs and one targeted oligonucleotide silencer of splicing (TOSS)[14] were designed for each splicing event, and we scored their effect on the phenotype of the SKOV3ip1 ovarian cancer cell line using multiplexed fluorescent dyes for cell count, viability and apoptosis assays (**Supplementary Figs. 1** and **3**). We carried out the assays in biological and technical triplicates and calculated quality metrics (*Z* factors) for each assay plate (**Supplementary Figs. 1** and **3**). Phenotypic defects reproduced by at least two independent isoform specific inhibitors (ISIs) against the same splicing event with a robust *Z* score of >3 were considered functionally relevant and retained for further analysis.

As expected, mock transfection or transfection of an unrelated siRNA or TOSS did not affect the cellular phenotypes, whereas transfection of an siRNA against the positive control transcript, encoding RNA-binding motif 8A (*RBM8A*), consistently induced apoptosis and reduced cell counts and viability (**Supplementary Fig. 3**). Although most of the targeted splicing events did not have any phenotypic effect (*Z* score <3), four splicing events in the genes encoding anterior gradient homolog-3 (*AGR3*), fibronectin-1 (*FN1*), myeloid cell leukemia sequence-1 (*MCL1*) and spleen tyrosine kinase (*SYK*) produced robust apoptosis induction (**Supplementary Table 2**). We were unable to validate ISI-dependent changes in the expression of *AGR3* by PCR because of this gene's low expression level, and thus it was not pursued further.

The remaining three genes affecting apoptosis have previously been implicated in cell-survival pathways[15,16]. Inhibiting the expression of the long isoforms of these three genes by siRNA resulted in a three- to eight-fold increase in the ratio of apoptotic marker–positive cells (**Fig. 2**, left, and **Supplementary Table 2**). Similarly, we observed 4-fold to 12-fold increases in the ratio of propidium iodide–positive, nonviable cells by siRNA-mediated silencing of the long isoforms of these three genes (**Fig. 2**, left, **Supplementary Table 2**). Consistently, reprogramming *FN1* extra-domain B (*FN1*-EDB) and *SYK* splicing using TOSS resulted in increased apoptosis and decreased viability (**Fig. 2a** and **Supplementary Table 2**). In contrast, modulation of *MCL1* alternative splicing with TOSS had a modest effect on apoptosis (**Fig. 2b**). Silencing of the genes encoding cyclin E1 (*CCNE1*) and ligase IV (*LIG4*) by splice isoform–specific siRNA produced marked decreases in cell viability (*Z* scores >3; **Supplementary Table 2**) but did not result in substantial apoptosis (**Supplementary Table 2** and data not shown). Overall, the screen results indicate that 10% of the ASEs tested contribute to the viability of cancer cells *in vitro*.

Inhibition of tumor-associated variants induces apoptosis

The phenotypic effects we observed could be due to changes in alternative splice forms or to a general reduction in gene expression. To differentiate between these two effects, we compared the impact of siRNA and TOSS silencing on global and isoform-specific expression. Global siRNAs equally inhibited the expression of constitutive, long and short splice isoforms of *SYK*, *MCL1* and *FN1* (**Fig. 2**, right). Isoform-specific siRNAs inhibited the accumulation of the long, but not the short, splice isoforms, while proportionally reducing the overall gene expression. In contrast, reprogramming splicing with TOSS simultaneously reduced expression of the long splice isoform and increased expression of the short splice isoform to various extents for *SYK* and *MCL1* transcripts without altering overall mRNA levels (**Fig. 2**, right). TOSS against *FN1*-EDB decreased expression of the EDB+FN1 isoform while concomitantly decreasing the overall *FN1* transcript level. Notably, although decreasing the overall expression of these genes failed to trigger apoptosis, inhibiting the expression of the long splice isoforms of all three genes induced apoptosis by four- to eight-fold (**Fig. 2**, left), confirming the results of the high-content screen. Reprogramming the splicing of *SYK* with TOSS consistently induced apoptosis (**Fig. 2a**, left, white bars). TOSS targeting *FN1*-EDB produced apoptosis by decreasing the long EDB+ isoform and global *FN1* expression, thus behaving in a manner similar to an isoform-specific siRNA (**Fig. 2c**). A second TOSS that modulated the *FN1*-EDB splicing ratio without decreasing overall *FN1* expression did not produce apoptosis (data not shown). TOSS targeting *MCL1* did not induce apoptosis, despite a substantial increase in RNA corresponding to the short isoform (**Fig. 2b**).

The inability of TOSS targeting *MCL1* to induce apoptosis suggests that either the change in the splicing ratio of *MCL1* is not sufficient to induce apoptosis or TOSS-induced changes in *MCL1* mRNA expression do not lead to corresponding changes in protein isoforms. To differentiate between these two possibilities, we performed western blotting against *MCL1* in cells transfected with *MCL1* ISIs or control ISIs. *MCL1* isoform–specific siRNAs diminished the expression of the long MCL1 protein (**Supplementary Fig. 4a**). However, *MCL1* TOSS did not change the level of the long MCL1 protein isoform, nor did it increase the short protein isoform (**Supplementary Fig. 4a**). Therefore, TOSS against *MCL1* fails to induce apoptosis because it does not change the ratio of the corresponding protein isoforms, suggesting

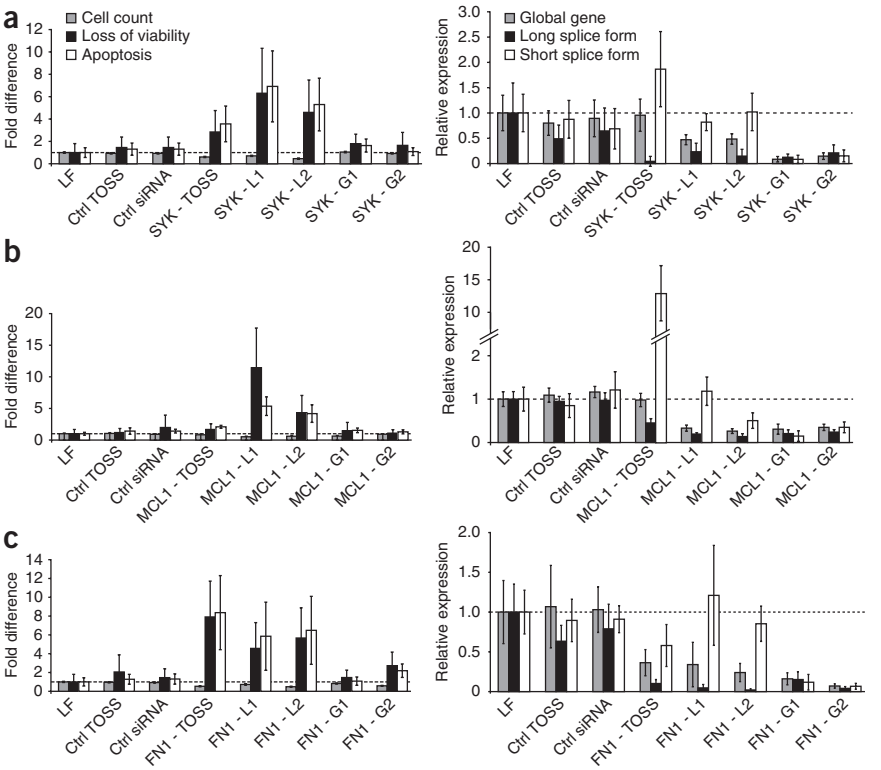

Figure 2 Targeting of *SYK*, *MCL1* or *FN1*-EDB alternatively spliced isoforms induces apoptosis. (**a**–**c**) The impact of TOSS and siRNAs targeting the pre-mRNAs encoding SYK (**a**), MCL1 (**b**) and FN1 (**c**) proteins on cellular phenotype (left) and RNA expression monitored by qPCR (right) were evaluated and compared to that in mock-transfected (LF) SKOV3ip1 ovarian cancer cells. Experiments were performed in three biological and three technical replicates, and an average for each cellular phenotype was calculated for each ISI. Left, the impact of TOSS and alternative exon–specific siRNAs (L1, L2) on cell count (gray), loss of viability (black) and apoptosis (white) are shown as bar graphs. Right, the qPCR relative expression values for the overall gene expression (gray), long splice isoform (black) and short splice isoform (white) are indicated. Error bars represent the s.d. of the replicates. siRNA and TOSS with unrelated sequences were used as negative controls (Ctrl). The three genes shown were analyzed with a full set of ISIs and siRNAs that inhibit global gene expression (G1, G2).

the existence of mechanisms that compensate for changes in the RNA expression of this gene in the cell line tested. Indeed, *MCL1* transcripts are known to be extremely unstable, and the MCL1 protein has a rapid turnover of about 30 min[17]. Furthermore, exon skipping of *MCL1* produces a frameshift that results in a premature stop codon, thus making this message susceptible to nonsense-mediated decay and highly unstable[18]. In support of this, we failed to detect any endogenous MCL1 protein bands corresponding to the short isoform, even following TOSS treatment (**Supplementary Fig. 4a**). We also could not verify levels of the different FN1-EDB protein isoforms because of their large size (>220 kDa), which prevented their separation by SDS-PAGE (data not shown), and the absence of suitable isoform-specific antibodies. Consequently, we focused our studies on *SYK* and did not pursue the analysis of *FN1* and *MCL1* any further.

To verify whether the *SYK* ISI-induced RNA splicing shifts had an impact at the protein level, we carried out western blot analyses using antibodies against SYK proteins following treatment with different ISIs or control oligonucleotides (**Fig. 3** and **Supplementary Fig. 4b**). Addition of global siRNAs against constitutively spliced *SYK* exons decreased the levels of all protein isoforms, whereas siRNA against the long *SYK* isoform decreased the expression of the long but not the short protein isoform. In contrast, treatment of the cells with TOSS reduced the expression of the long and increased the expression of the short protein isoform of SYK (**Fig. 3a** and **Supplementary Fig. 4b**). Successful modulation of *SYK* alternative splicing was associated with enhanced cleavage of the apoptosis marker PARP, confirming the specific impact of alternative splicing on apoptosis (**Supplementary Fig. 4b**).

We also investigated the effects of *SYK* splicing modulation in various normal and cancer cell lines expressing different levels and splicing isoform ratios of *SYK* RNA, to evaluate the specificity of the observed effects on apoptosis. As expected, transfection of *SYK*-specific ISIs into cells that do not express *SYK* (for example, MDA-MB231 and Hs578t breast cancer cell lines) or normal cells (that is, MCF-10A mammary epithelial cells or BJ-Tielf fibroblasts) did not promote apoptosis (data not shown and **Supplementary Fig. 5c**). In contrast, cells showing the same *SYK* splice isoform ratio as observed in cancer tissues (for example, HCT116 colorectal carcinoma and TOV-112D endometrioid carcinoma cells) entered into apoptosis upon the modulation of *SYK* alternative splicing (**Supplementary Fig. 5a**,**b**). We conclude that the alternative splicing of cancer-associated genes can specifically influence cancer cell viability and apoptosis, in a manner that is largely independent of the overall level of gene expression.

Alternative splicing of *SYK* controls cell cycle and mitosis

Previous reports suggested that *SYK* splice isoforms are localized differently in the cell[19,20]. Therefore, we investigated the possibility that changes in *SYK* alternative splicing induce apoptosis by changing the cellular localization of the protein. We fractionated the cytoplasmic and nuclear proteins following treatment with different *SYK* ISIs, and carried out western blotting to detect the SYK protein isoforms. In untreated cells, the long SYK isoform, SYK(L), was predominantly nuclear and the short isoform, SYK(S), was predominantly cytoplasmic (**Fig. 3a**). Treatment of the cells with ISIs reduced the expression of the long isoform of SYK in the nucleus, and most SYK proteins became cytoplasmic. This suggests that altering the cellular localization of the protein may induce apoptosis.

To determine whether the effect of SYK alternative splicing is limited to the regulation of apoptosis and cell survival or extends to other known *SYK* cellular activities such as cell proliferation, we monitored the impact of the ISIs on cell-cycle progression. Upon close visual examination of cell images from SKOV3ip1 cells treated with *SYK* ISIs, we noted an increased amount of cells displaying abnormal nuclear morphology with larger, aberrant nuclei, and of cells bearing two or more nuclei (**Fig. 3b**,**c**), indicating that SYK(L) is involved in mitotic exit and cytokinesis. Changing the alternative splicing of *SYK* led to an accumulation of cells in the G2–M phase of the cell cycle (**Fig. 3d**), which is consistent with defective mitosis. The mitotic arrest was confirmed by the increase in phospho-histone H3 (**Fig. 3c**). This mitotic arrest was isoform specific, as we did not observe it following general *SYK* knockdown with global siRNAs (**Fig. 3d**). Notably, *SYK* TOSS produced the opposite effect to that of SYK siRNAs, that is, TOSS caused a decrease in abnormal mitosis and phospho-histone H3

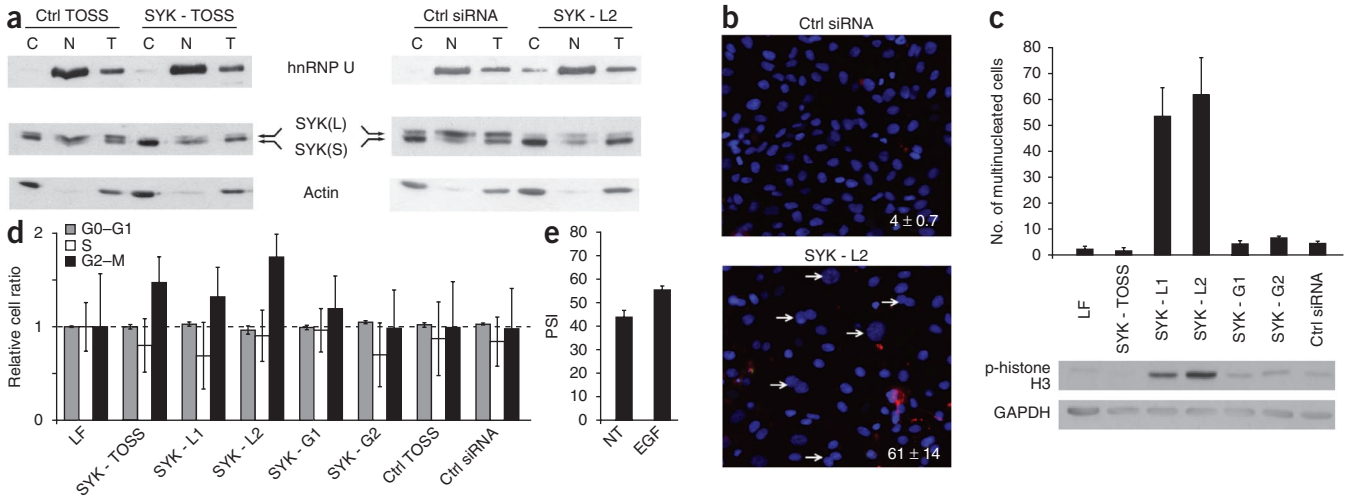

Figure 3 SYK alternative splicing regulates cell-cycle progression and mitosis. (**a**) Reducing the expression of the long SYK splice isoform induces the accumulation of the SYK protein in the cytoplasm. Cells were treated by the different ISIs, the nuclei (N) and cytoplasm (C) were separated using differential extraction and centrifugation, and proteins were extracted and visualized by western blotting. Total cellular proteins (T) were also loaded as reference. The nuclear splicing factor hnRNP U and the cytoplasmic protein actin were used as fractionation markers. SYK(L) and SYK(S) indicate the position of the long and short splicing isoforms of SYK, respectively. (**b**) Inhibiting the expression of SYK(L) isoform induces changes in nuclear morphology. The cells were treated with control (Ctrl) siRNA or SYK(L) siRNA as indicated, and nuclei were stained with Hoechst 33342 dye 96 h after transfection. The nonviable cells were stained with propidium iodide. Arrows indicate abnormal or supernumerary nuclei. The numbers in the bottom of each image indicate the average numbers of abnormal nuclei ± s.d. observed per treatment. (**c**) SYK alternative splicing regulates mitosis and cytokinesis. Images from cells transfected with SYK ISIs or control ISIs were inspected visually, and cells with abnormal mitosis or supernumerary nuclei were counted and plotted as bar graphs. The numbers are the average of three independent transfections. Below, western blotting of the same samples with a phospho-histone H3 antibody, a known mitosis marker[45]. (**d**) SYK alternative splicing regulates progression through the G2–M phase of the cell cycle. The cell-cycle distribution of SKOV3ip1 cells 48 h after transfection with different ISIs was analyzed using flow cytometry. The accumulation of transfected cells in G0–G1 phases (gray), S phase (white) and G2–M phase (black) relative to that of untreated cells is shown as a bar graph. The data are an average of three independent transfection experiments and error bars represent the s.d. (**e**) EGF promotes SYK(L) exon inclusion. The bar graph shows the changes in SYK splicing upon EGF treatment. PSI values were calculated as described[11]. Error bars represent the s.d. from three independent treatments.

levels (**Fig. 3c**), suggesting that increasing the expression of the short *SYK* isoform can compensate for the long isoform–dependent effect on mitosis.

Given the importance of mitogenic signaling in oncogenesis and cell proliferation, we investigated the effect of oncogenic growth factors on *SYK* splicing. We observed the pro-survival alternative splicing pattern of SYK *in vitro* upon exposure to epidermal growth factor (EGF, **Fig. 3e**), which is known to promote cell proliferation and differentiation, underscoring the role of alternative splicing in regulating the activity of this gene. Therefore, we conclude that cancer cell mitosis is regulated by both the amount and the ratio of *SYK* splicing isoforms.

SYK(L) isoform induces JUN-dependent cell survival

To understand how *SYK* alternative splicing promotes malignant growth, we used quantitative PCR (qPCR) to test the impact of the different *SYK* ISIs on the expression of a panel of genes involved in apoptosis, the cell cycle and cancer. Reducing the expression of the long isoform of *SYK* resulted in prominent increases in the expression of JUN[21], as measured by qPCR in SKOV3ip1 cells (**Supplementary Table 3**). Notably, we observed this result when targeting the expression of the long *SYK* isoform by either siRNA or TOSS, but not when the overall expression of *SYK* was downregulated by siRNA against constitutive exons (**Supplementary Table 3**). This suggests

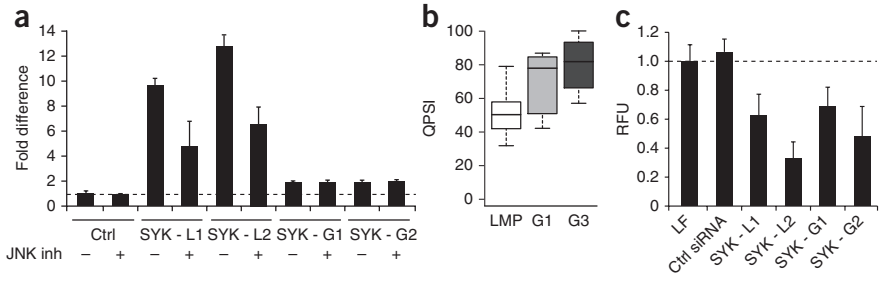

Figure 4 SYK(L) promotes malignancy and anchorage-independent growth. (**a**) SYK alternative splicing regulates JUN-dependent cell survival. SKOV3ip1 cells were transfected with siRNAs targeting SYK(L). After 24 h, cells were treated with the JNK inhibitor SP600125 or a DMSO control (Ctrl). The cells were allowed to grow for 72 h and, subsequently, apoptotic cells were stained with annexin-V, as in **Figure 2a**. Results represent the average of three individual experiments. (**b**) Expression of SYK(L) splice isoform is a marker for tumor malignancy. The ratio of SYK splice isoforms was monitored by qPCR in RNA extracted from six borderline (LMP), grade 1 (G1) or grade 3 (G3) ovarian tumors. The percent splicing index (qPSI) was calculated as described[12] and the relative values are presented as box plots. (**c**) Altering the alternative splicing pattern of SYK inhibits anchorage-independent growth. SYK ISI–transfected SKOV3ip1 cells, or cells transfected with control ISIs, were seeded in 96-well plates containing soft agar and incubated for 7 d in order to form colonies. Cells were subsequently stained with Hoechst 33342 and total fluorescence was measured and plotted against ISI controls. The time frame of the assay precluded the use of the TOSS. Error bars represent s.d. of three independent experiments. RFU, relative fluorescence units.

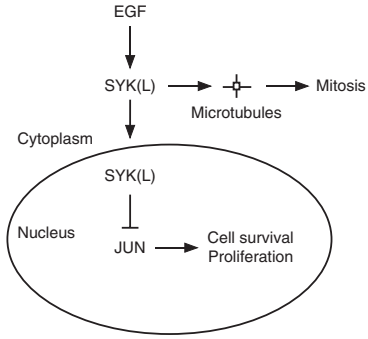

Figure 5 A model of the different functions of the SYK(L) pro-survival isoform. Extracellular growth factors such as EGF activate signal transduction pathways. The EGF signal promotes a splicing shift in the SYK long isoform, which affects SYK protein isoform subcellular localization and activities. SYK(L) can have at least two distinct functions depending on its cellular location: it can either enter the nucleus where it normally represses JUN expression and promotes cell survival, or in the cytoplasm it can associate with the centrosome and microtubules, where it is essential for mitotic spindle assembly and cytokinesis.

that changing the splicing pattern of *SYK* and not the global expression affects the MAPK–JNK signaling pathway that acts as a conduit for apoptosis[22].

To directly test this hypothesis, we evaluated the effect of the JNK inhibitor SP600125 (ref. 23) on SYK-induced apoptosis. The inhibition of JNK with SP600125 partly rescued the apoptosis induced by modulation of SYK(L) isoform expression in SKOV3ip1 cells (**Fig. 4a**), indicating that the SYK-induced phenotype is mediated at least in part by JUN activation. We conclude that the production of SYK(L) by alternative splicing promotes JNK-dependent cell survival.

SYK(L) promotes tumor malignancy

Our results suggest that increased expression of the *SYK* long isoform in tumors may increase not only cell survival but also cellular proliferation and tumor aggressiveness. To test this hypothesis, we monitored *SYK* splicing in a total of 18 ovarian cancer tissues from tumors of low malignant potential (LMP), grade 1 tumors (G1) and the aggressive grade 3 tumors (G3). Consistent with the idea that *SYK* regulates tumor aggressiveness, the expression of the *SYK* long isoform was higher in G1 tumors than in in LMP tissues, and higher still in G3 tumors (*P* value between LMP and G3 = 0.001; **Fig. 4b**). To further dissect the mechanism by which *SYK* splicing promotes aggressive tumor growth, we monitored the impact of silencing the SYK(L) isoform on anchorage-independent growth *in vitro*. The ability of SKOV3ip1 cells to form colonies in soft agar was markedly inhibited in the presence of siRNAs against the long isoform or against both long and short isoforms (**Fig. 4c**). This indicates that—unlike the impact of *SYK* on apoptosis and mitosis, which requires a minimum expression of the short isoform—the effect on tumorigenesis is influenced by the expression level of only the long form, independent of the splicing ratio. We conclude that the expression level of the *SYK* long splicing isoform regulates tumor aggressiveness by promoting anchorage-independent growth and cell proliferation.

Splicing regulation is a common feature of the MAPK–JNK pathway

To determine whether alternative splicing–dependent regulation of gene function is limited to *SYK* or extends to other members of the MAPK–JNK pathway, we tested the functional impact of all cancer-associated ASEs[5] in this pathway. We examined a list of all cancer-associated splicing events in genes with ontology terms related to phosphoinositide-3 kinase (PI3K) signal transduction or MAPK–JNK (http://palace.lgfus.ca/link/pheno_screen_pi3k-akt) for function *in vitro* as described in **Figure 1**. From this, we identified 13 cancer-associated isoforms (see http://palace.lgfus.ca/link/mapk-jnk_annotation for an annotation table) and validated previously undefined isoform-specific function for the MAP3K7 (TAK1) and MINK1 kinases. In both cases, silencing the long splicing isoform of these two genes reduced cell viability by inducing apoptosis in SKOV3ip1 cells (**Supplementary Fig. 6**). We conclude that alternative splicing has a crucial role in modulating the production of isoforms of players regulated by the MAPK/JNK pathway.

DISCUSSION

In this study we have presented a procedure for evaluating the functional impact of alternative splicing on phenotypic parameters that are relevant to cancer. Moreover, we have uncovered cancer-specific alternative splicing events that promote cell proliferation and survival. Approximately 10% of all tested breast cancer–associated and ovarian cancer–associated splicing events significantly affected cell viability *in vitro*, confirming that splicing pattern changes in cancer are not simply an inconsequential anomaly of diseased cells, but instead may have been selected for functional advantages.

The strongest effect we observed on apoptosis resulted from inhibiting the expression level of the long isoform of *MCL1*, a member of the *BCL2* mitochondrial apoptotic regulator family. MCL1 is primarily localized to the outer mitochondrial membrane, where it promotes cell survival by interacting with other Bcl-2 family members[24]. Active MCL1 promotes cell viability by inhibiting the activation of caspases, leading to apoptosis. MCL1 has a short half-life because of its regulation at multiple levels, including alternative splicing, allowing the rapid induction by survival signals or elimination of the protein by apoptotic signals[25]. Alternative splicing leads to skipping of MCL1 exon 2 and deletion of the C-terminal transmembrane domain, resulting in protein mislocalization to the cytosol[24].

Our results suggest that apoptosis is regulated by the expression level of the long isoform of MCL1 (**Fig. 2** and **Supplementary Fig. 4a**). This observation is somewhat different from the results of earlier experiments, which showed that overexpression of the MCL1 short isoform, which lacks the pro-survival transmembrane and BH2 domains, causes apoptosis[18,26]. In our hands, apoptosis was induced upon decreasing the expression level of the long isoform, even when the expression of the short isoform was not detectable by western blotting (**Supplementary Fig. 4a**). This suggests that apoptosis is not strictly dependent on increasing the amount of the short isoform. Apoptosis was not induced to the same levels by siRNAs against constitutive exons compared with those targeting the long isoform. However, close inspection of the level of knockdown suggests that global inhibition in these experiments did not reduce the amount of the long isoform to the same degree observed with the long isoform–specific siRNA (**Supplementary Fig. 4a** and data not shown). Once again, the results are consistent with a long isoform–specific effect on apoptosis. Indeed, inhibition of the MCL1 long isoform by itself in skin cancer cell lines was also shown to cause apoptosis[27]. Therefore, in the case of MCL1, apoptosis seems to be regulated at least in part by changes to the expression level of the long isoform.

In addition to regulating the splicing of apoptotic genes, tumorigenesis also impairs apoptosis by altering the splicing of kinases such as SYK[28]. We have found that ovarian tumors preferentially express the long isoform of SYK. Intriguingly, SYK is required for leukemic B-cell proliferation and survival through regulation of MCL1 expression[15,16]. This isoform was previously reported to affect the

subcellular distribution of the SYK protein kinase via a nonclassical nuclear localization signal (NLS) located in the alternative exon[19]. Indeed, our data show that the SYK(L) isoform is nuclear, and changes in SYK splicing affect its nuclear localization, consistent with these observations. In addition, we find that modulation of SYK splicing causes cell-cycle perturbations and defective mitosis.

The involvement of SYK in cell proliferation and mitotic progression has been documented in breast cancer cells[29,30]. Furthermore, SYK has been shown to localize to the centrosomes, where it associates with γ-tubulin[31]. SYK is also found in microtubules[32] and it phosphorylates α-tubulin[33], thus providing a possible explanation for why changing the splicing of this gene impairs mitosis. However, the mechanism by which SYK splicing exerts its effect on apoptosis seems to be mediated by the activity of c-JUN. The expression of this protein, which regulates the cell cycle and apoptosis[22], was found to be modified upon changing SYK splicing (**Supplementary Table 3**). In addition, the SYK isoform–dependent apoptotic phenotype was rescued in the presence of JNK inhibitors, underlining the importance of c-JUN expression for the induction of SYK-dependent apoptosis. Together, the results are consistent with a model in which cancer cells promote cell survival by inducing the expression of the SYK pro-survival isoform, which in turn suppresses the expression of c-JUN and its target genes, thereby inhibiting apoptosis (**Fig. 5**).

SYK acts as a tumor suppressor in breast cancer, and loss of its expression is required for malignant growth and tumor cell invasion[29]. Paradoxically, SYK can also act as an oncogene in other types of tumors, and SYK overexpression has been associated with T-cell lymphomas[34] and chronic leukemias[35] as well as gastric cancer[36] and head and neck carcinomas[37], in which its expression correlates with tumor progression and has prognostic value. These contradictory expression profiles of SYK in different tumor types are difficult to explain based on global gene expression. Confusion about the role of SYK in different cancers may be due in part to the methods used in these studies to evaluate the expression and the functional impact of SYK, because no distinction was made between the global and splice isoform–specific increase in SYK expression. It is possible that differential expression of SYK(L) and SYK(S) may contribute to these disparate observations in different cancers.

In support of this, Wang and co-workers[19] observed elevated SYK(S) expression in human breast carcinomas, but not in matched normal mammary tissues, suggesting a role for SYK(S) in mammary tumor progression. Consistent with a role for SYK alternative splicing in tumorigenesis, Goodman *et al.* have observed aberrant SYK splicing in childhood acute B-cell leukemias[38]. Alternatively, the differences in SYK behavior in different cancer types may be due to differences in the contribution of SYK to tumor biology. In this study, we have found that whereas apoptosis is affected only by changes in the splicing pattern of SYK (**Fig. 2a**), mitosis and cell proliferation are affected by changes in both SYK splicing and expression (**Fig. 3**). In contrast, anchorage-independent growth (**Fig. 4c**) is driven mostly by overall SYK expression and not splicing. Accordingly, tumors that depend on SYK for viability will be mostly dependent on SYK splicing and its impact on c-JUN, which is cell-type specific, whereas those tumors that use SYK to modulate cell adhesion will be mostly affected by changes in the overall expression level of SYK. In our hands, we found that ovarian cancer and colorectal cancer cell lines are most sensitive to changes in SYK splicing whereas invasive breast cancer cell lines generally do not express SYK[29] and therefore are not sensitive to SYK modulation *in vitro* (**Supplementary Figure 5** and data not shown). Indeed, SYK splicing pattern was linked to ovarian and not breast cancer *in vivo*[11,12]. In all cases, our observations underline the need to re-examine previously established links between SYK gene expression and tumor behavior, with a clear distinction between isoform and global changes in gene expression.

The functional contribution of alternative splicing to cancer cell biology reported here is not static but responds to extracellular signals. Indeed, we observed increased exon inclusion in *SYK* and *FN1*-EDB alternative exons with short-term EGF treatment (**Fig. 3e**). This finding is consistent with previous reports indicating that *FN1* alternative splicing is regulated by growth factors through the phos PI3K-AKT and Ras signal transduction pathways[39]. The effect of EGF on alternative splicing of SYK and FN1 is likely to be mediated by splicing modulators such as proteins of the serine–arginine-rich (SR) or heterogeneous nuclear ribonucleoproteins (hnRNP) families[40]. Indeed, knocking down hnRNP-K in SKOV3ip1 cells changes the splicing pattern of these genes and promotes apoptosis (**Supplementary Fig. 7**). Notably, EGF has been reported to regulate hnRNP-K expression and activity[41], suggesting that the effect of EGF on *SYK* and *FN1* alternative splicing could be mediated by hnRNP-K.

Components of the exon junction complex have recently been shown to regulate MAPK splicing and EGF signaling in *Drosophila melanogaster*[42,43]. It is therefore tempting to speculate on the existence of an additional layer of complexity involving alternative splicing in the EGF–Ras signaling axis that has functional consequences in tumor progression (**Supplementary Fig. 8**). Indeed, we found that apoptosis is induced by alteration of the splicing of the *MAP3K7* and *MINK* genes, both part of the MAPK cell survival pathway and previously linked to ovarian and breast cancers[5] and to Ras-induced growth arrest in ovarian epithelial cells[44], respectively. On the basis of these data, we propose that splicing acts as a modulator of cancer cell survival or cell death by regulating the EGF–MAPK–JNK pathway. It is also important to note that the impact of alternative splicing on the cell survival pathway is likely to be stronger than reported in this study, as the functional effect of many splicing events associated with cancer *in vivo* might be missed owing to the limited conditions and cell types that can be sampled *in vitro*.

METHODS

Methods and any associated references are available in the online version of the paper at http://www.nature.com/nsmb/.

Note: Supplementary information is available on the Nature Structural & Molecular Biology website.

ACKNOWLEDGMENTS

We are indebted to C. Rancourt (Département de Microbiologie, Université de Sherbrooke) for providing cell lines and help in the initial setup phase of the project and to B. Lamontagne and L. Bergeron Jr. for assay setup and help with troubleshooting. We thank the Réseau de Recherche sur le Cancer (Fonds de la Recherche en Santé du Québec; FRSQ) tissue bank for ovarian tumor tissues and L. Volkov for help with flow cytometry. This work was funded by Genome Canada/Génome Québec and National Cancer Institute of Canada grant no. 700529. B.C. is the Canada Research Chair in Functional Genomics. J.-P.P. is the Canada Research Chair on Genomics and Catalytic RNA. S.A.E. is a Chercheur National of the FRSQ.

AUTHOR CONTRIBUTIONS

D. Garneau, M.B., D. Gendron., S.C., J.-P.B., E.L. and M.D. carried out experiments and analyzed data and J.-F.L., P.T. and J.G.-B. analyzed data and prepared the figures. J.-F.L. developed the ISI design program and the FASE statistics and bioinformatics analysis tools. J.-P.B., K.T., E.L. and P.T. developed the qPCR procedures used to evaluate ISI impact on splicing. H.N. did the histopathological review of tissue specimens. P.P., K.T., R.K., J.-P.P., B.C., R.J.W. and S.A.E. designed experiments, discussed data and participated in the writing of the paper. P.P. and K.T. supervised experiments and analyzed data. P.P. and S.A.E. wrote the manuscript.

COMPETING FINANCIAL INTERESTS
The authors declare no competing financial interests.

Published online at http://www.nature.com/nsmb/.
Reprints and permissions information is available online at http://npg.nature.com/reprintsandpermissions/.

1. Pan, Q., Shai, O., Lee, L.J., Frey, B.J. & Blencowe, B.J. Deep surveying of alternative splicing complexity in the human transcriptome by high-throughput sequencing. *Nat. Genet.* **40**, 1413–1415 (2008).
2. Wang, E.T. *et al.* Alternative isoform regulation in human tissue transcriptomes. *Nature* **456**, 470–476 (2008).
3. Matlin, A.J., Clark, F. & Smith, C.W. Understanding alternative splicing: towards a cellular code. *Nat. Rev. Mol. Cell Biol.* **6**, 386–398 (2005).
4. Castle, J.C. *et al.* Expression of 24,426 human alternative splicing events and predicted *cis* regulation in 48 tissues and cell lines. *Nat. Genet.* **40**, 1416–1425 (2008).
5. Venables, J.P. *et al.* Cancer-associated regulation of alternative splicing. *Nat. Struct. Mol. Biol.* **16**, 670–676 (2009).
6. Venables, J.P. Aberrant and alternative splicing in cancer. *Cancer Res.* **64**, 7647–7654 (2004).
7. Cooper, D.L. & Dougherty, G.J. To metastasize or not? Selection of CD44 splice sites. *Nat. Med.* **1**, 635–637 (1995).
8. Christofk, H.R. *et al.* The M2 splice isoform of pyruvate kinase is important for cancer metabolism and tumour growth. *Nature* **452**, 230–233 (2008).
9. Levanon, E.Y. & Sorek, R. The importance of alternative splicing in the drug discovery process. *Targets* **2**, 109–114 (2003).
10. Iorns, E., Lord, C.J., Turner, N. & Ashworth, A. Utilizing RNA interference to enhance cancer drug discovery. *Nat. Rev. Drug Discov.* **6**, 556–568 (2007).
11. Klinck, R. *et al.* Multiple alternative splicing markers for ovarian cancer. *Cancer Res.* **68**, 657–663 (2008).
12. Venables, J.P. *et al.* Identification of alternative splicing markers for breast cancer. *Cancer Res.* **68**, 9525–9531 (2008).
13. Celotto, A.M. & Graveley, B.R. Exon-specific RNAi: a tool for dissecting the functional relevance of alternative splicing. *RNA* **8**, 718–724 (2002).
14. Villemaire, J., Dion, I., Elela, S.A. & Chabot, B. Reprogramming alternative pre-messenger RNA splicing through the use of protein-binding antisense oligonucleotides. *J. Biol. Chem.* **278**, 50031–50039 (2003).
15. Baudot, A.D. *et al.* The tyrosine kinase Syk regulates the survival of chronic lymphocytic leukemia B cells through PKCdelta and proteasome-dependent regulation of Mcl-1 expression. *Oncogene* **28**, 3261–3273 (2009).
16. Gobessi, S. *et al.* Inhibition of constitutive and BCR-induced Syk activation downregulates Mcl-1 and induces apoptosis in chronic lymphocytic leukemia B cells. *Leukemia* **23**, 686–697 (2009).
17. Adams, K.W. & Cooper, G.M. Rapid turnover of mcl-1 couples translation to cell survival and apoptosis. *J. Biol. Chem.* **282**, 6192–6200 (2007).
18. Bingle, C.D. *et al.* Exon skipping in Mcl-1 results in a bcl-2 homology domain 3 only gene product that promotes cell death. *J. Biol. Chem.* **275**, 22136–22146 (2000).
19. Wang, L. *et al.* Alternative splicing disrupts a nuclear localization signal in spleen tyrosine kinase that is required for invasion suppression in breast cancer. *Cancer Res.* **63**, 4724–4730 (2003).
20. Zhou, F., Hu, J., Ma, H., Harrison, M.L. & Geahlen, R.L. Nucleocytoplasmic trafficking of the Syk protein tyrosine kinase. *Mol. Cell. Biol.* **26**, 3478–3491 (2006).
21. Shaulian, E. AP-1—the Jun proteins: oncogenes or tumor suppressors in disguise? *Cell. Signal.* **22**, 894–899 (2010).
22. Wisdom, R., Johnson, R.S. & Moore, C. c-Jun regulates cell cycle progression and apoptosis by distinct mechanisms. *EMBO J.* **18**, 188–197 (1999).
23. Bennett, B.L. *et al.* SP600125, an anthrapyrazolone inhibitor of Jun N-terminal kinase. *Proc. Natl. Acad. Sci. USA* **98**, 13681–13686 (2001).
24. Akgul, C. Mcl-1 is a potential therapeutic target in multiple types of cancer. *Cell. Mol. Life Sci.* **66**, 1326–1336 (2009).
25. Michels, J., Johnson, P.W. & Packham, G. Mcl-1. *Int. J. Biochem. Cell Biol.* **37**, 267–271 (2005).
26. Bae, J., Leo, C.P., Hsu, S.Y. & Hsueh, A.J. MCL-1S, a splicing variant of the antiapoptotic BCL-2 family member MCL-1, encodes a proapoptotic protein possessing only the BH3 domain. *J. Biol. Chem.* **275**, 25255–25261 (2000).
27. Shieh, J.J., Liu, K.T., Huang, S.W., Chen, Y.J. & Hsieh, T.Y. Modification of alternative splicing of Mcl-1 pre-mRNA using antisense morpholino oligonucleotides induces apoptosis in basal cell carcinoma cells. *J. Invest. Dermatol.* **129**, 2497–2506 (2009).
28. Mócsai, A., Ruland, J. & Tybulewicz, V.L. The SYK tyrosine kinase: a crucial player in diverse biological functions. *Nat. Rev. Immunol.* **10**, 387–402 (2010).
29. Coopman, P.J. *et al.* The Syk tyrosine kinase suppresses malignant growth of human breast cancer cells. *Nature* **406**, 742–747 (2000).
30. Moroni, M. *et al.* Progressive loss of Syk and abnormal proliferation in breast cancer cells. *Cancer Res.* **64**, 7346–7354 (2004).
31. Zyss, D. *et al.* The Syk tyrosine kinase localizes to the centrosomes and negatively affects mitotic progression. *Cancer Res.* **65**, 10872–10880 (2005).
32. Faruki, S., Geahlen, R.L. & Asai, D.J. Syk-dependent phosphorylation of microtubules in activated B-lymphocytes. *J. Cell Sci.* **113**, 2557–2565 (2000).
33. Peters, J.D., Furlong, M.T., Asai, D.J., Harrison, M.L. & Geahlen, R.L. Syk, activated by cross-linking the B-cell antigen receptor, localizes to the cytosol where it interacts with and phosphorylates alpha-tubulin on tyrosine. *J. Biol. Chem.* **271**, 4755–4762 (1996).
34. Feldman, A.L. *et al.* Overexpression of Syk tyrosine kinase in peripheral T-cell lymphomas. *Leukemia* **22**, 1139–1143 (2008).
35. Buchner, M. *et al.* Spleen tyrosine kinase is overexpressed and represents a potential therapeutic target in chronic lymphocytic leukemia. *Cancer Res.* **69**, 5424–5432 (2009).
36. Nakashima, H. *et al.* Clinical significance of nuclear expression of spleen tyrosine kinase (Syk) in gastric cancer. *Cancer Lett.* **236**, 89–94 (2006).
37. Luangdilok, S. *et al.* Syk tyrosine kinase is linked to cell motility and progression in squamous cell carcinomas of the head and neck. *Cancer Res.* **67**, 7907–7916 (2007).
38. Goodman, P.A., Wood, C.M., Vassilev, A., Mao, C. & Uckun, F.M. Spleen tyrosine kinase (Syk) deficiency in childhood pro-B cell acute lymphoblastic leukemia. *Oncogene* **20**, 3969–3978 (2001).
39. Blaustein, M. *et al.* Concerted regulation of nuclear and cytoplasmic activities of SR proteins by AKT. *Nat. Struct. Mol. Biol.* **12**, 1037–1044 (2005).
40. Shin, C. & Manley, J.L. Cell signalling and the control of pre-mRNA splicing. *Nat. Rev. Mol. Cell Biol.* **5**, 727–738 (2004).
41. Mandal, M. *et al.* Growth factors regulate heterogeneous nuclear ribonucleoprotein K expression and function. *J. Biol. Chem.* **276**, 9699–9704 (2001).
42. Ashton-Beaucage, D. *et al.* The exon junction complex controls the splicing of MAPK and other long intron-containing transcripts in *Drosophila*. *Cell* **143**, 251–262 (2010).
43. Roignant, J.Y. & Treisman, J.E. Exon junction complex subunits are required to splice *Drosophila* MAP kinase, a large heterochromatic gene. *Cell* **143**, 238–250 (2010).
44. Nicke, B. *et al.* Involvement of MINK, a Ste20 family kinase, in Ras oncogene-induced growth arrest in human ovarian surface epithelial cells. *Mol. Cell* **20**, 673–685 (2005).
45. Hendzel, M.J. *et al.* Mitosis-specific phosphorylation of histone H3 initiates primarily within pericentromeric heterochromatin during G2 and spreads in an ordered fashion coincident with mitotic chromosome condensation. *Chromosoma* **106**, 348–360 (1997).

ONLINE METHODS

Cell culture and transfection. All cell lines were cultured in antibiotic- and antimycotic-free medium (Wisent). The ovarian adenocarcinoma SKOV3ip1 cell line was grown in DMEM/F12 (50/50) medium supplemented with 10% (v/v) FBS and 2 mM L-glutamine. TOV112D endometrioid carcinoma cells and HCT116 colorectal adenocarcinoma were propagated in OSE medium or McCoy's modified 5a medium (Wisent), respectively, supplemented with 10% (v/v) FBS and 2 mM L-glutamine. Cell propagation and passaging were as recommended by the American Type Culture Collection (ATCC). Recombinant human EGF (Pepro-Tech) was used at 50 ng ml^{-1} for the EGF induction experiment. For image analyses and RNA extractions, SKOV3ip1 cells were seeded in 96-well tissue culture–treated imaging plates (BD Biosciences) at a density of 5,000 cells per well. For immunoblotting and fluorescence-activated cell sorting (FACS) analyses, cells were seeded at 350,000 cells per well in six-well plates (BD Biosciences). Transfections were performed in suspension using Lipofectamine 2000 (Invitrogen) according to the manufacturer's protocol and 10 nM of 21-mer siRNA duplexes or 400 nM of TOSS oligonucleotides with 2-OMe chemical modifications (IDT). Each oligonucleotide was transfected in randomly positioned wells in triplicate (technical replicates) on at least three different transfection dates (biological replicates). The transfection efficiencies were confirmed by transfecting a fluorescent AlexaFluor 488–conjugated negative control siRNA (AllStars siRNA, Qiagen) in every plate. For the rescue experiments, JNK inhibitor II (SP600125, EMD Biosciences) was added 24 h after transfection at a final concentration of 10 μM.

Small interfering RNA and targeted oligonucleotide silencer of splicing oligonucelotide design. To design long isoform–specific siRNA and TOSS, we used an algorithm identifying the alternatively included region[46]. All possible stretches of 19 nt (siRNA) or 20 nt (TOSS) were extracted and scored (**Supplementary Fig. 2**). The top-scoring siRNAs and TOSS were used for the FASE screen. Refer to http://palace.lgfus.ca/data/related/1059 for all sequences. To perform global gene knockdown using siRNA, a global gene junction-ranking algorithm was developed (J.F.L., unpublished).

RNA extraction and quantitative PCR. Total RNA extractions were performed in 96-well plates with the Absolutely RNA Microprep Kit (Stratagene) as recommended by the manufacturer, except that DNase treatments were done at 37 °C. RNA quality and the presence of contaminating genomic DNA were verified as described[46]. RNA integrity was assessed for 11 random samples per 96-well plate with an Agilent 2100 Bioanalyzer. Reverse transcription was performed at 55 °C on a fixed volume (5.5 μl) of RNA sample with Transcriptor (Roche Diagnostics), random hexamers, dNTPs and 10 units of RNaseOUT (Invitrogen) in a total volume of 10 μl. All cDNAs were diluted by adding 65 μl of RNase DNase-free water. Quantitative PCR reactions were performed on 1 ng cDNA as described[46]. Relative expression levels were calculated using the qBASE framework[47] using *PSMC4* and *SDHA* as reference genes. Primer design and validation were evaluated as described[46]. Additionally, an algorithm was developed to design primer pairs targeting constitutive exon junctions of a given gene and were tested as described[46]. In every run, a no-template control and a no–reverse transcription control (no RT) on a mock-transfected sample were performed for each primer pair. These controls were consistently negative.

Apoptosis, viability and cell enumeration triplex assay. A 96-well multiplex assay was performed to simultaneously monitor viability, apoptosis and cell count in each well. Cells were stained 96 h after transfection with the following three fluorescent dyes: 1 μg ml^{-1} of propidium iodide (Invitrogen), 1:350 of annexin V–Alexa Fluor 647 (Invitrogen) and 800 ng ml^{-1} of Hoechst 33342 (Invitrogen) in an annexin-binding buffer (pH 7.4) composed of 10 mM HEPES, 140 mM NaCl and 2.5 mM $CaCl_2$. High-content endpoint fluorescence images were acquired on a BD Pathway 855 BioImager (BD Biosciences) using a 20× objective with a laser-based auto focus and excitation and emission filters appropriate for each fluorescent dye. Experimental error was reduced with the acquisition of nine images (800 μm gap between each frame) per well per dye. Image pre-processing and segmentation were performed with Attovision 1.6 software (BD Biosciences). Thresholds were applied manually to identify propidium iodide and annexin V positive cells.

Soft agar colony formation assay. SKOV3ip1 cells were seeded at 5,000 cells per well and transfected in 96-well tissue culture–treated plates. At 24 h after transfection, the cells were trypsinized and seeded in a 1.2% agar base layer (MJS BioLynx) containing DMEM/F12 supplemented with 20% (v/v) FBS and 4 mM L-glutamine. Once the cell layer was solidified, 100 μl of medium was added to each well and the plates were incubated for 7 d at 37 °C under 5% CO_2. On the seventh day, medium was removed, and the cells were stained for 1 h with Hoechst 33342 (5 μg ml^{-1}). Fluorescence was measured on a FLX800 microplate fluorescence reader (BioTek Instruments).

Immunoblotting. Cells were collected from six-well plates 72 h after transfection, pooled and lysed as described[48]. Refer to **Supplementary Methods** for the conditions and the antibodies used.

Statistical analysis and quality-control metrics. A pilot screen was used to establish the dynamic range and robustness of the assay with *Z*-factor scores routinely in excess of 0.5 (**Supplementary Fig. 3**). The *Z* factor[49] was determined by calculating the average and s.d. of the randomly distributed triplicate wells of the positive-control *RBM8A* versus the Lipofectamine control wells for each plate.

Data processing and hit identification. The primary screening assay produced a multiplex readout of cell count, viability and apoptosis by a combination of three vital dyes (**Fig. 1**). Triplicate technical replicates of triplicate biological transfections were performed. A complete randomization of the plate was used each time to eliminate systematic instrument measurement errors (**Supplementary Fig. 1**). All valid plates were normalized by comparing to lipofectamine treatment (**Supplementary Fig. 9**). A stringent statistical cut-off of 3 median absolute deviations[50,51] above the median measurements per assay (corresponding to a robust *Z* score >3) was used to minimize false positives and ensure true-positive phenotypes[50]. This method is robust to outliers and can identify weak hits and is thus deemed ideal for RNAi screens[50]. All the steps for data processing, normalization and hit calling are outlined in **Supplementary Figure 9**.

46. Brosseau, J.P. *et al.* High-throughput quantification of splicing isoforms. *RNA* **16**, 442–449 (2010).
47. Hellemans, J., Mortier, G., De Paepe, A., Speleman, F. & Vandesompele, J. qBase relative quantification framework and software for management and automated analysis of real-time quantitative PCR data. *Genome Biol.* **8**, R19 (2007).
48. Venables, J.P. *et al.* Multiple and specific mRNA processing targets for the major human hnRNP proteins. *Mol. Cell. Biol.* **28**, 6033–6043 (2008).
49. Zhang, J.H., Chung, T.D. & Oldenburg, K.R. A simple statistical parameter for use in evaluation and validation of high throughput screening assays. *J. Biomol. Screen.* **4**, 67–73 (1999).
50. Birmingham, A. *et al.* Statistical methods for analysis of high-throughput RNA interference screens. *Nat. Methods* **6**, 569–575 (2009).
51. Chung, N. *et al.* Median absolute deviation to improve hit selection for genome-scale RNAi screens. *J. Biomol. Screen.* **13**, 149–158 (2008).

doi:10.1038/nsmb.2040